

Research article

Nutrient Recovery from Poultry Wastewater by Modified Biochar: An Optimization Study

Nguyen Lan Thanh^{1,2}, Vo Thanh Hang^{1,2}, Nguyen Thi Thuy^{2,3}, Lam Pham Thanh Hien^{1,2} and Nguyen Nhat Huy^{1,2*}

¹Faculty of Environment and Natural Resources, Ho Chi Minh City University of Technology (HCMUT), 268 Ly Thuong Kiet St., Dist. 10, Ho Chi Minh City, Vietnam

²Vietnam National University Ho Chi Minh City, Linh Trung Ward, Thu Duc District, Ho Chi Minh City, Vietnam

³School of Chemical and Environmental Engineering, International University, Quarter 6, Linh Trung Ward, Thu Duc City, Ho Chi Minh City, Vietnam

Received: 10 November 2022, Revised: 28 December 2022, Accepted: 4 April 2023

DOI: 10.55003/cast.2023.06.23.013

Abstract

Keywords

biochar;
adsorption;
ammonia;
phosphate;
crop residues

In this work, we proposed and tested a method for utilizing agricultural waste and alum sludge as an effective adsorbent to treat poultry wastewater. The product was also targeted to be used as fertilizer for agriculture. Modified biochar was produced from crop residues, sludge from a water treatment plant, and magnesium salt. The produced biochar was characterized by scanning electron microscopy, energy-dispersive X-ray spectroscopy, Brunauer-Emmett-Teller analysis, and X-ray diffraction. The adsorption of ammonia and phosphate in both synthetic and actual poultry wastewater by the produced biochar was conducted. The effect of experimental conditions such as N to P ratio, initial concentrations of ammonium and phosphate, pH, and the amount of biochar on the adsorption capacity for ammonia and phosphate were also investigated. The results from the experiment showed that the best adsorption capacities were 60.64 mgNH₄⁺-N/g and 66.24 mgPO₄³⁻-P/g, which were produced at the optimum conditions of N to P ratio of 1.25, initial concentration of 90 mg/L, pH 6, and biochar mass of 0.105 g. These results create an opportunity for the effective production of slow-release fertilizer from crop residues and alum sludge for ecological agriculture in the future.

*Corresponding author: Tel.: (+84) 901964985

E-mail: nnhuy@hcmut.edu.vn

1. Introduction

With the increase in population, the consumption of pork, beef, or chicken has gone up rapidly around the world, especially in developing countries like Vietnam. This has led to the growth of the livestock industry with about 4.58 million tons of meat produced in 2014. The livestock industry has brought a lot of negative effects on the environment [1]. Approximately 80 million tons of animal waste per year were reported by the Ministry of Agriculture and Rural Development, and about 80% of it was discharged from small farms and large farms [2, 3]. Besides, there were nearly 36% of this 80% discharged directly into the environment without any treatment [2]. On a long term, the discharge of this animal waste will seriously harm the environment. Moreover, the total production from henneries increased by about 6% per year, of which chicken production accounted for about 1.45 (76.03% of poultry) million tons and egg production of about 10.8 billion tons (61.75% of total poultry egg) [2]. Poultry wastewater usually contains 16-165 mg/L of NH_4^+ -N, 16-32 mg/L of PO_4^{3-} -P, 78.5% of TS (e.g., Mg and Na), and high organics (BOD and COD) [4-7]. Phosphate (PO_4^{3-}) and ammonia (NH_4^+) are the two basic components of total phosphorus and total nitrogen found in wastewater [1]. A high concentration of these compounds can lead to eutrophication where phosphorus and nitrogen become nutrients nourishing the algae growth in water. The thick algae layer covers surface water and prevents sunlight and oxygen from entering the water, creating turbidity and an anoxic environment in which underwater animals die off due to the inadequacy of oxygen [1, 8]. In addition, N and P are important resources for agricultural uses. The world's total minable P reserves are limited and unevenly distributed [9, 10]. Even though commercial P resources for agricultural use are typically anticipated to be depleted in the next 50-100 years, and P demand is progressively growing at a rate of 2.5% per year, and is expected to surpass supply by 2035 globally [10]. N is a vital prerequisite for the development of life. Although N_2 may be fixed abundantly by biological nitrogen absorption, the process is sluggish and insufficient to supply the broad world N requirement for crops [10]. Therefore, the recovery of the N and P from wastewater should be of more concern at present.

Recently, various technologies for the treatment of poultry wastewater that contains nitrogen and phosphorous, including chemical method and biological methods have been developed [1, 11]. However, most chemical methods are expensive due to the high amount of chemicals used [11]. In the case of biological treatment, it is hard to maintain a suitable environment for the microorganism [11]. At present, cleaner production is of more concern than end-of-pipe treatment, and therefore we should find a greener way to treat wastewater, recover the nutrients and produce high-value products. Among the solutions, biochar as an adsorbent emerges as one of the best options for cleaner production. Vietnam is an agriculture country, so crop residues produced annually are huge. Almost 80% of crop residues were thrown out or incinerated [3, 12]. Besides, the sludge from the wastewater treatment plants or water supply treatment plants contains a large amount of N and P, which is typically not used productively [13]. In addition, both crop residues and water treatment sludge can be used as raw materials for biochar production [13].

Biochar is a carbon material produced from biomass with a cheap production price, which can be used as environment-friendly material for soil reclamation [11, 14, 15]. Biochar can be manufactured by various methods such as pyrolysis, gasification, carbonization, and hydrothermal [16]. Biochar offers several benefits when used for soil or pollutant adsorption. However, modified biochar was studied to maximize its utility [17]. A problem with biochar is that its production via biomass pyrolysis often produces material that is powdery and of small particle size and is hard to remove from solution [15, 18]. Many scientists have focused on combining metal oxides with granular biochar via chemical co-precipitation. Additionally, the scientists felt that by using the correct approach, the modified biochar might then have enhanced surface area, surface charge, or more functional groups on sorption sites. As a result, biochar modification often involves increasing

pore volume and surface area, improving surface characteristics, and incorporating new elements into the biochar matrix, generating advantageous composites [18]. Moreover, modification of biochar can be done by different techniques such as physical modification, chemical modification, biochar metal oxide combination, chemical reagent use, pyrolysis-impregnation, and co-precipitation [15, 19]. Nonetheless, some findings demonstrated that biochar derived from phosphate-rich biomass tended to slowly release phosphorus into solution rather than adsorb it [20]. For the recovery of biochar as a fertilizer after treatment, chemical co-precipitation was an effective choice [20]. Furthermore, the ratio of Mg to N and P equal to 1 was used to form a precipitation known as struvite [21-23]. Some metal salts (e.g., calcium, magnesium, and aluminum) were successfully used as agents for nutrient recovery but the cost of these metals was not affordable for the economy [24-26]. MgO or CaO were used for nutrient recovery because of their alkaline characteristics and because they were environmentally friendly metals, but the metal oxides lacked adsorption ability for dissolved organic substances. Besides, biochar might not adsorb phosphate and anions so the combination of metal oxides such as MgO and biochar should be investigated [21, 25, 27].

There were several researchers who studied fabricating biochar from crop residues or sludge to remove N and P from wastewater. Corn biochar was used for adsorbing phosphorous from swine wastewater and MgO-impregnated sugarcane biochar was used for removing N and P [11, 14]. Mg-biochar from poplar chips was utilized for removing N and P and MgO-biochar from wood waste was used as valuable fertilizer [22, 23]. Moreover, Mg-biochar from sewage sludge ash was produced and applied in the recovery of phosphorous and nitrogen from water [28]. Santhosh *et al.* [29] used two types of biomass, wooden chip and sewage sludge separate, as magnetic biochar to investigate the differences between modified and unmodified biochar with Fe_2O_3 for the removal of Cr(VI), and acid orange 7 dye. Additionally, some other related examples of application of biomass were MgCl_2 -P. australis biochar [30, 31], sewage sludge ash and willow [31], MgCl_2 -rice straw [21], Mg-phosphorus rich biochar [27], MgCl_2 -corn stalk [32], Mg-biochar/bentonite composite bead [33], and Mg/Ce-wheat corn straw [34]. These studies gave an idea for combining both crop residues (low nutrient and ash) and alum sludge (low carbon and surface area, high aromatic hydrocarbon and metal) [31] from a water treatment plant as an adsorbent for the recovery of N and P from poultry wastewater. This idea was intended to solve four problems: (i) water pollution from poultry wastewater, (ii) agricultural waste from crop residues, (iii) solid waste from water supply treatment sludge, and (iv) the need for green fertilizer for use in agricultural soils in Vietnam, which has not been reported in the literature.

In this study, crop residues and water supply sludge were co-pyrolyzed for biochar fabrication. The biochar was then impregnated with $\text{MgCl}_2 \cdot 6\text{H}_2\text{O}$ and used as an adsorbent for the recovery of N and P from poultry wastewater. The effect of environmental factors on the N and P adsorption in synthetic wastewater was investigated. An experimental design was applied to optimize the adsorption conditions, and the adsorbent was then tested with actual poultry wastewater.

2. Materials and Methods

2.1 Material preparation and characterization

Crop residues (i.e., sugarcane, coffee ground, tea leaves, and rice husks) were collected from around Ho Chi Minh City (Vietnam), and alum sludge was collected at the Tan Phu Ground Water Treatment Plant (Ho Chi Minh City, Vietnam).

The procedure for material preparations was referenced from previous reports [13, 14]. The residues and sludge were dried at 105°C and cut or ground into small pieces of sizes 0.15 - 0.4 mm. The materials were then heated at 500°C for 1 h in the case of the sludge and 30 min for the crop residues. Next, 5 g of the mixture of each residue and sludge at a weight ratio of 50:50 were shaken at 120 rpm with 250 mL of 10% MgCl₂ solution for 3 h. The mixtures were then dried at 80°C in an oven until complete evaporation. Each mixture was finally dried at 106°C for 6 h and then heated at 550°C for 1 h. The produced materials (named biochar) were stored in a zipper bag and desiccant cabinet, which were named based on the raw biomass material used, BS for bagasse + sludge, CS for coffee ground + sludge, TS for tea leaves + sludge, and RS for rice husk + sludge.

The surface morphologies of the produced biochar samples were observed with scanning electron microscopy (SEM) while the surface elemental distributions and the compositions of the materials were determined by Energy-dispersive X-ray spectroscopy (EDX) (JEOL JSM-IT200). The crystalline structure of the material was examined by X-ray diffraction (XRD, Bruker D2 Phaser).

2.2 Adsorption experiment

Synthetic wastewater was prepared from KH₂PO₄ and NH₄Cl salts dissolved in double-distilled water. First, 100 mL of synthetic wastewater in 250-mL Erlenmeyer flasks were prepared at pH 6, NH₄⁺ concentration of 75 mg/L, N/P ratio of 1.25, and biochar dosage of 0.12 g/L, to determine the most effective type of biomass (bagasse, coffee ground, tea leaves, rice husk) and sludge. After the best biochar was determined, the optimum adsorption conditions for recovery of ammonium and phosphate was obtained using the Design-Expert experimental design software for synthetic poultry wastewater [5-7, 35, 36]. The tested range of conditions was 5-9 for pH, 0.10-0.12 g/100 mL for biochar dosage, 60-100 mg/L for NH₄⁺, and 1-2 for N/P ratio. The synthetic wastewater experiments for the most effective biomass were replicated about three times, while the optimum values for synthetic and actual wastewater were repeated six times like the CCD model. The adsorption capacity (Q_e , mg/g) of the ammonium and phosphate was calculated using the equation below.

$$Q_e = \frac{(C_o - C) \times V}{m}$$

Where C_o and C (mg/L) are the initial and equilibrium concentrations, respectively. V (L) is the volume of the solution and m (g) is the amount of biochar.

Each water sample was filtered through filter paper (110Φ Newstar 102) before analyzing ammonia and phosphate concentration. Ammonia was analyzed following the TCVN 5988:1995 using a distillation device (BUCHI Unit K-355) and phosphate was analyzed following the TCVN 6202:2008 using a spectrophotometer (HACH DR-6000).

3. Results and Discussion

3.1 Preliminary test and material characterization

Figure 1 demonstrates the adsorption of phosphate and ammonia using four types of biochar with and without sludge. The adsorption capacities for phosphate without sludge of bagasse, coffee ground, tea leaves, and rice husk were 43.25, 10.53, 40.19, and 11.73 mgPO₄³⁻-P/g, respectively, while the adsorption capacity of ammonium for the same biochar were 29.52, 25.48, 31.39, and 28.59 mgNH₄⁺-N/g, respectively. However, when this biochar was combined with sludge from the

supply water treatment plant, the adsorption capacity of ammonium raised significantly to 37.30, 37.92, 35.43, 40.41 mgNH₄⁺-N/g, respectively, and those for phosphate to 47.13, 42.76, 47.90, and 42.68 mgPO₄³⁻-P/g, respectively. It might be explained by the presence of aromatic groups or metallic elements in the sludge that helped in promoting the active sites and surface areas of the biochar responsible for adsorbing ammonium and phosphate [10, 27, 29, 37]. This observation was consistent with the results of Kończak and Huber [31] who found that sewage sludge ash and willow had the highest ammonium adsorption capacity of about 36.6 mg/g. However, in the case of phosphate adsorption, the sewage sludge alone had the more effective adsorption capacity of 88.1 mg/g.

The most effective biomass precursor for phosphate recovery was tea leaves, followed by bagasse with adsorption capacities of 47.13±2.69 and 47.90±0.65 mgPO₄³⁻-P/g, respectively. In comparison, the study of Xu *et al.* with the MgO sugarcane bagasse biochar had a phosphate adsorption capacity of > 35 mgP/g (with an initial concentration of 61 mgPO₄³⁻-P/L) [38], while that of Takaya *et al.* [39] using Fe (II) sugarcane bagasse biochar had a high removal efficiency of 97%. Besides, the ammonium adsorption capacities of rice husk-sludge and bagasse-sludge were higher than the others with 40.41±2.034 and 37.30±2.12 mgNH₄⁺-N/g, respectively. Additionally, Jiang *et al.* [30] prepared banana straw and cassava straw modified by MgCl₂ with an adsorption capacity of 24.04 mg/g for ammonium and 31.15 mg/g for total phosphorous which was mainly caused by the Mg precipitation with ammonium and phosphate [10, 30]. Therefore, MgO-modified bagasse and sludge biochar (named BS biochar) was the most effective biochar for the recovery of ammonium and phosphate and it was more economically viable than the others, it was chosen to be used in the further investigations and characterizations.

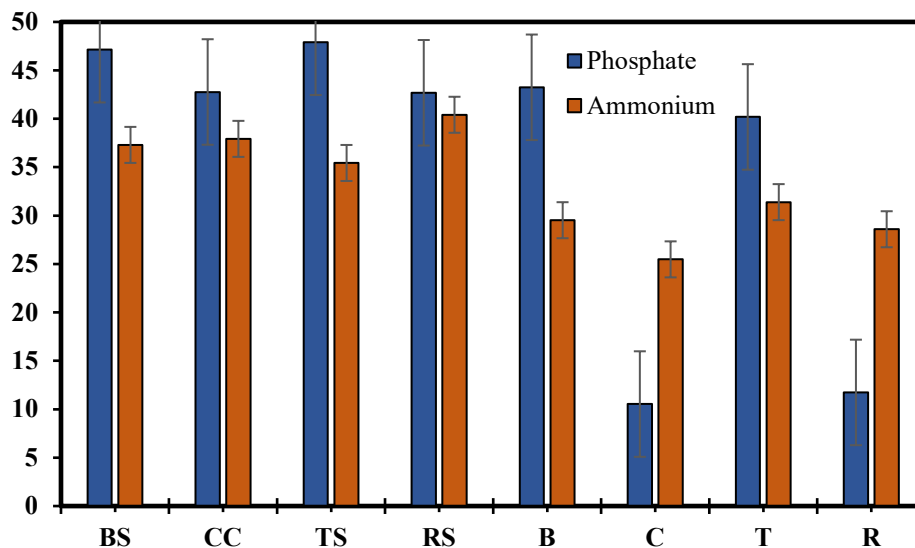


Figure 1. Ammonium and phosphate adsorption capacity of different types of biochar

The surface morphologies of the raw materials (bagasse and sludge) and BS biochar obtained from SEM analysis are illustrated in Figure 2. The raw bagasse had a smooth surface with some tiny pores with sizes of < 1 μm while the sludge had a rough surface, comprised of many small sludge particles with pore sizes of ≥ 1 μm. After being impregnated with MgCl₂·6H₂O, the MgO-

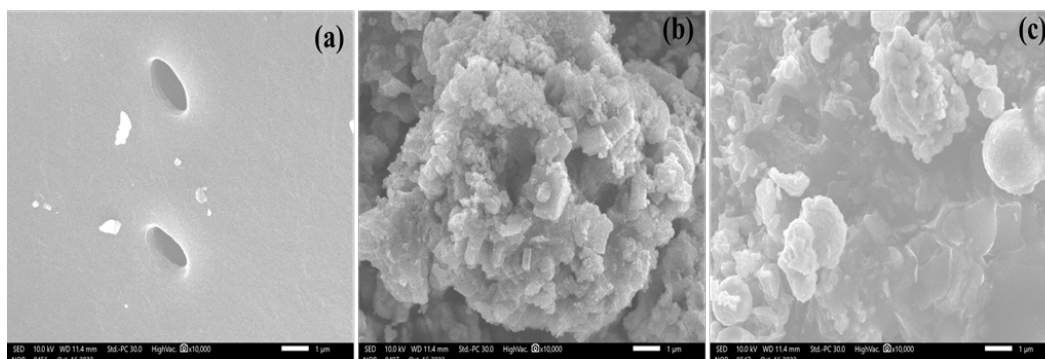


Figure 2. SEM images of raw material and modified biochar: (a) raw bagasse, (b) raw sludge, (c) BS biochar (bagasse and sludge with MgCl_2) (magnification: $\times 10,000$)

modified biochar had a rough flaky, and uneven surface. The flakes of MgO on the surfaces helped enhance the pore size [27, 33, 40]. Raw materials containing organic compounds were carbonized to form biochar, while $\text{MgCl}_2 \cdot 6\text{H}_2\text{O}$ was severely dehydrated at 550°C to generate MgO flakes on the surface of the produced biochar. These SEM images were consistent with the study of Yin *et al.* [22] and Li *et al.* [14] which the flake of MgO distribution on the biochar surface.

With the flake of MgO on the surface of biochar and the angle view in SEM images, it seems hard to exactly determine the pore size. Therefore, BET surface analysis was conducted for determining surface area and pore volume. The specific surface area of BS biochar was about $171.251 \text{ m}^2/\text{g}$ with a pore volume of $0.267 \text{ cm}^3/\text{g}$. This was comparable with other research on the specific surface area such as wood biochar and rice husk biochar (57.1 and $4.38 \text{ m}^2/\text{g}$) [41], corncob ($23.3 \text{ m}^2/\text{g}$) [42, 43], rape ($184 \text{ m}^2/\text{g}$) [43, 44], Chinese cabbage ($124 \text{ m}^2/\text{g}$) [43, 45, 46], peanut straw ($99.1 \text{ m}^2/\text{g}$) [44, 45], rice husk ($273.6 \text{ m}^2/\text{g}$), and wood ($11 \text{ m}^2/\text{g}$) [43]. Moreover, other research on various biochar materials indicated specific surface area and pore volumes of sugarcane bagasse by MgCl_2 soaking ($1440.4 \text{ m}^2/\text{g}$ and $1.574 \text{ cm}^3/\text{g}$) [47], oilseed rape straw by co-pyrolysis of coal gangue ($144.59 \text{ m}^2/\text{g}$ and $0.069 \text{ cm}^3/\text{g}$) [48], sludge by slow pyrolysis ($1.850 \text{ m}^2/\text{g}$) [49], sludge by dewatering with Fenton and slow pyrolysis ($4.890 \text{ m}^2/\text{g}$) [49], and sewage sludge by pyrolysis under CO_2 ($109 \text{ m}^2/\text{g}$ and $0.085 \text{ cm}^3/\text{g}$) [50]. Overall, the BS biochar (bagasse and sludge with MgCl_2) at 550°C was successfully synthesized and had quite a good specific surface area and pore volume compared with other studies.

Figure 3 illustrates the desorption and adsorption on the surface of BS biochar. The Figure correlates to a typical Type IV adsorption isotherm and Type C hysteresis loop (de Boer's five types of hysteresis) [51, 52]. In Type IV adsorption, mesopores and macropores with an average pore size of $1.5 \sim 100 \text{ nm}$ were developed [52-54]. At low pressures, the material had the same trend as Type II which developed nonporous or microporous. At first, it was adsorbed in a monolayer, and then a multilayer [52, 54, 55], and after that capillary condensation occurred in the material's pore at high pressures [51, 52].

EDX analysis was used to characterize the chemical composition of MgO -modified biochar before and after the adsorption of NH_4^+ and PO_4^{3-} . Figure 4 shows the peaks of chemical substances in modified biochar with their percentage compositions before and after adsorption. After being impregnated with MgO , it can be clearly seen the presence of Mg in the fresh BS biochar before adsorption at about 47% (Figure 4a), indicating that the MgO -modified biochar had been successfully fabricated. For comparison with other research, the Mg content in coffee ground bean/3M MgO and palm tree trunk/3M Mg was 9.36 and 11.05%, respectively [28]. In the study of

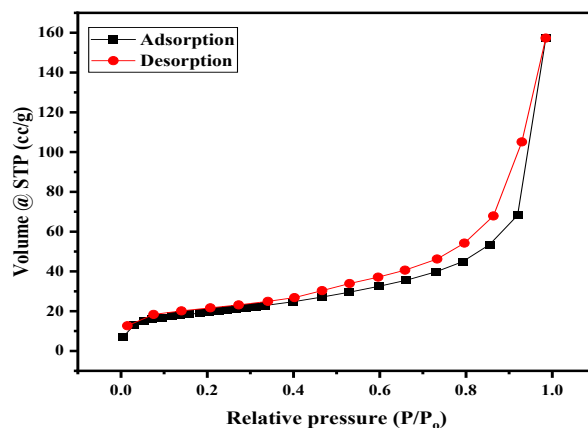


Figure 3. The adsorption and desorption isotherms of the BS biochar

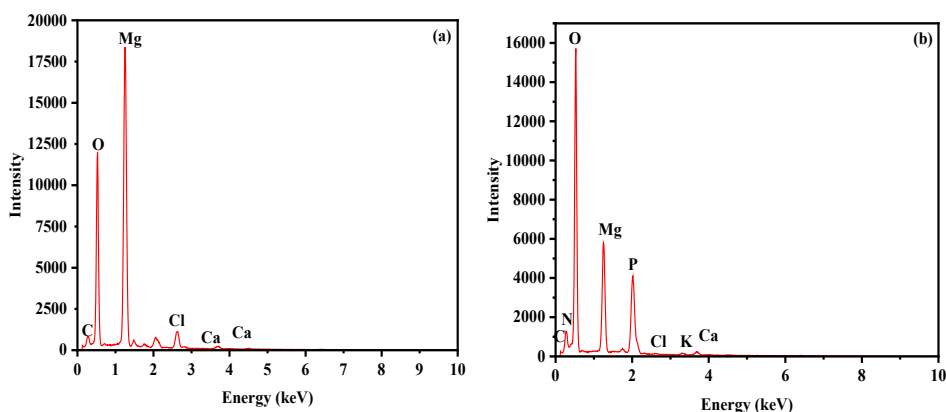


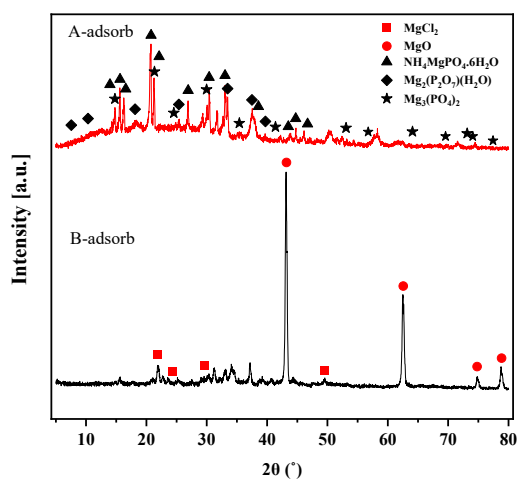
Figure 4. EDX results of BS biochar (a) before and (b) after adsorption

Li *et al.* [14], Mg content was 23.94% in sugarcane/MgO 20%. Furthermore, in our study, the sample after adsorption had N and P at 1.04 and 21.13 % (w/w), respectively, showing that the biochar was effectively recovering N and P. Other compounds in biochar such as CaCO_3 and KCl did not change into other forms or affect the modified biochar except for increasing the amount of carbon content in the biochar [14]. In Table 1, the decline of Mg percentage in EDX results was evidence of precipitation between Mg-N-P [27, 28, 56-59]. Furthermore, the presence of N and P after adsorption verified the adsorption ability of this material.

The XRD patterns in Figure 5 describe the formation of struvite from Mg, P, and N. Moreover, the surface charges of Mg can reduce the chances of NH_4^+ adsorption [23, 28]. It can be seen that the peaks of MgO at 2θ of 44.4° , 64° , 75° , and 79° (JCPDS: 30-0794) [32] in the biochar confirm the presence of MgO particles on the BS biochar [28, 60]. From this evidence and the percentage of Mg in the EDX results, it can be concluded that the Mg was loaded successfully on the material. At pH range of 4-10, the main species in solution were HPO_4^{2-} and H_2PO_4^- with negative charges while Mg sites were positively charged [56]. This favors the formation of struvite,

Table 1. The elemental percentage by EDX analysis in the BS biochar before and after adsorption

Elements	Before Adsorption		After Adsorption	
	Mass %	Atom %	Mass %	Atom %
C	6.45±0.06	10.82±0.09	10.56±0.07	16.33±0.1
O	34.49±0.13	43.42±0.16	48.33±0.15	56.09±0.18
Mg	47.09±0.17	39.01±0.14	15.76±0.10	12.04±0.08
Cl	7.55±0.1	4.29±0.06	0.28±0.03	0.15±0.02
Ca	1.85±0.08	0.93±0.04	2.02±0.08	0.94±0.04
N	-	-	1.04±0.04	1.38±0.05
P	-	-	21.13±0.15	12.66±0.09
K	-	-	0.88±0.06	0.42±0.03

**Figure 5.** XRD patterns of BS biochar before and after adsorption

$\text{Mg}_3(\text{PO}_4)_2$, and $\text{Mg}_2(\text{P}_2\text{O}_7) \cdot (\text{H}_2\text{O})$, which was successfully confirmed by the XRD results [14, 61]. The XRD pattern displays strong peaks at 2θ of 15° , 15.5° , 15.8° , 20.9° , 21.5° , 25.2° , 30.6° , 31.9° , 33.3° , 37° , 44.5° , and 46.3° , which were consistent with other studies [21, 25, 27, 32, 33]. This means that the adsorption mechanism of ammonium and phosphate might be precipitation as struvite with Mg on the biochar surface.

3.2 Optimization results

The experiment was conducted with Design Expert (DE) 11 software using response surface methodology (RSM) and central composite design (CCD), which was calculated as $2^k + 2k + n$ (with k number of factors, n number of centers replicated, $2k$ addition star points). The distance from the star point to the center was $\alpha = 2^{k/4} = 2$. All the experiments were conducted at 5 levels ($-\alpha$, -1 , 0 , $+1$, $+\alpha$). This study had 6 center replicated points, 30 runs, and 8 experiments as additional points from the star point to the center point. Table 2 illustrates the experiment design from DE software.

Table 2. Experimental rank and level of independent variables

Factor	Name	Unit	-2(- α)	-1	0	+1	+2(+ α)
A	pH	-	5	6	7	8	9
B	N/P	-	1	1.25	1.5	1.75	2
C	Biochar dosage	mg/100mL	100	105	110	115	120
D	Initial concentration	mg/L	60	70	80	90	100

Table 3 illustrates the variance analysis result of the model for NH_4^+ and PO_4^{3-} adsorption capacity after insignificant factor removal. The adjusted and predicted R^2 values of both NH_4^+ and PO_4^{3-} adsorption capacity were 0.9049-0.8812 and 0.9966-0.9946, respectively, which were in reasonably agreement with a difference of less than 0.2. Therefore, the regression exactly described the data of experiments.

The F test from ANOVA (or Fisher test) in Table 3 shows the P value of ammonium and phosphate adsorption capacity $P_{\text{NH}_4^+} < 0.0001$ and $P_{\text{PO}_4^{3-}} < 0.0001$, respectively. This meant there was $< \frac{1}{100}$ a chance that an F value was largely due to noise. These results showed reasonable agreement with the predicted and actual values and was of high statistical reliability [62, 63].

The analysis of the fit of the model is also shown in Table 3. F test shows the lack of fit of the model by the comparison of the total variance of both actual and predicted values with the total variance of central replication point or the predictions of model miss observations. The results of the F test gave a P value > 0.05 ($P_{\text{NH}_4^+} = 0.1430$ and $P_{\text{PO}_4^{3-}} = 0.1705$), meaning that the hypothesis of “lack of fit” was insignificant, and the difference between two variances was not large [62]; therefore, the model was fitted. Furthermore, the coefficients of variation C.V.% for ammonium and phosphate adsorption capacities ($C.V_{\text{NH}_4^+} \% = 6.45$ and $C.V_{\text{PO}_4^{3-}} \% = 1.25$) were quite low, which indicated a high level of accuracy in the replication of experiments. All the results show the good fit of the model with the design of experiment. Equations (1) and (2) demonstrate the relationship between the adsorption capacity of NH_4^+ and PO_4^{3-} with 4 factors at encoding form (A = pH, B = N/P, C = Biochar dosage, D = Initial concentration).

Table 3. Analysis model fitting for experiments

Source	Model		Lack of fit		R^2	C.V. %	Adjusted R^2	Predicted R^2
	F value	P value	F value	P value				
Ion NH_4^+ Q_e (mg/g)	92.95	< 0.0001	2.63	0.1430	0.9147 \pm 0.556	6.45	0.9049	0.8812
Ion PO_4^{3-} Q_e (mg/g)	1417.63	< 0.0001	2.39	0.1705	0.9973 \pm 0.106	1.25	0.9966	0.9946

$$Q_e \text{ NH}_4^+ = 47.27 - 2.21B - 3.62C + 9.49D \quad (1)$$

$$Q_e \text{ PO}_4^{3-} = 44.85 - 8.16B - 2.14C + 6.74D - 0.7038BD + 1.66B^2 + 0.6770D^2 \quad (2)$$

The linear regression of equation 1 shows that the adsorption capacity of ammonium is affected by the first order of three factors B, C, and D. Besides, equation 2 shows the effect of first-order factors of B, C, D, pair of BD, and second order of B and D.

From equations 1 and 2, it can be concluded that the N/P ratio and biochar dosage has a negative effect on the adsorption capacity of both NH_4^+ and PO_4^{3-} , meaning that a rise in the ratio of N/P leads to a fall in the adsorption capacity of ammonium and phosphate. Besides, the biochar dosage and adsorption capacity have an inverse relationship. The struvite formation between Mg, NH_4^+ , and PO_4^{3-} has a percentage of 12% NH_4^+ and 58% PO_4^{3-} [57], which explains the reason for the inverted relationship between phosphate and N/P ratio. Moreover, an increase in initial concentration results in a growth of the adsorption capacity of both ammonium and phosphate, which is likely due to the high initial concentration creating a large chance for contact between biochar and ions of NH_4^+ and PO_4^{3-} ions. On the other hand, the level of pH was removed from the model. In more detail, the final solution pH always stayed the same at the range of 8-8.5 no matter what the initial pH of the solution was. Additionally, at a higher pH (> 9), NH_4^+ can be converted into NH_3 (gaseous), but at low pH, the H^+ and NH_4^+ can compete for the active sites on the biochar surface [32]. The point of zero charge of MgO was about 12. If the pH of the solution is lower than 12, the surface biochar charge is positive or otherwise [15, 64, 65]. It helps promote the adsorption capacity for phosphate by electrostatic attraction while the affinity for ammonium can be affected by affinity between inter negative charges of the biochar. Figure 6 depicts the 3D surface plots for the interaction between four factors and the adsorption capacity of ammonium and phosphate (mg/g). The relationship between ammonium and phosphate adsorption capacity with four factors was clearly indicated in these plots.

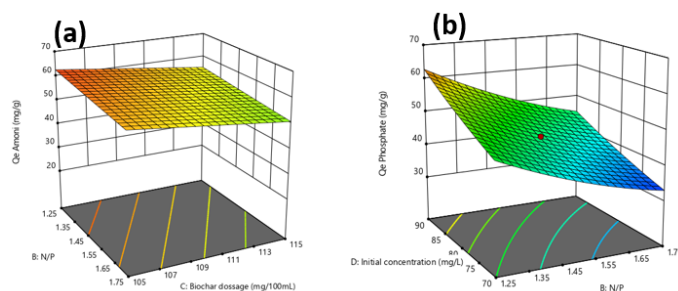


Figure 6. 3D surface plot of factors affecting adsorption capacity of (a) ammonium ion (NH_4^+) and (b) phosphate ion (PO_4^{3-}) using BS biochar

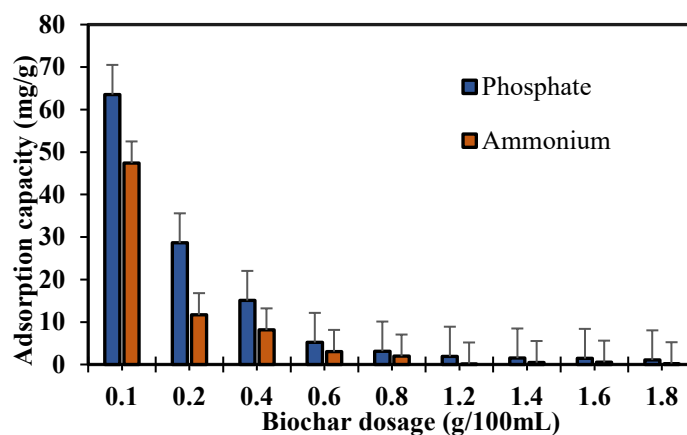
3.3 Application of optimized condition for synthetic and actual wastewater

Table 4 shows that the optimum values from the CCD design were: N/P ratio of 1.25, pH 6, biochar dosage of 0.105 g/100mL, and initial concentrations of 90 mg/L for NH_4^+ and 72 mg/L for PO_4^{3-} . The control experiment was replicated 6 times for accuracy with predicted values. From this Table, the actual values (60.64 mg NH_4^+ -N/g and 66.24 mg PO_4^{3-} -P/g) and predicted values (62.59 mg NH_4^+ -N/g and 64.93 mg PO_4^{3-} -P/g) were well in agreement with each other. For comparison, ammonium removal with modified biochar reports in the literature were: oak sawdust/ LaCl_3 (3.12 mg N/g with initial concentration 25.7 mg NH_4^+ /L [57, 66]), mixed hardwood (2.8 mg NH_4^+ /g with influent 980 mg NH_4^+ -N/g [67] and 0.48 mg PO_4^{3-} -P/g with phosphate concentration of 24 mg PO_4^{3-} -P/L), corn cob (1.09 mg NH_4^+ -N/g with 100 mg NH_4^+ -N/L) [40], unmodified sawdust (5.38 mg NH_4^+ -N/g) [65], unmodified sesame straw (26.84 mg NH_4^+ -N/g) [65, 68], corn stalk (37.72 mg NH_4^+ -N/g, 73.29 mg PO_4^{3-} /g)[32], and coal gangue modified oilseed rape straw (7.9 mg/ PO_4^{3-} -P g) [48]. MgO impregnation increases the adsorption effectiveness of the biochar, as observed for sugarcane [14], poplar chips [22], unmodified sawdust [65], unmodified sesame straw [65, 68], corn stalk [32], coal gangue modified oilseed rape straw [48], and brown marine macroalgae [69].

Table 4. Results of synthetic wastewater for testing the predicted model

	Actual Value (n=6)	Limits	Predicted Values	Difference (%)
$Q_e \text{ NH}_4^+$ ion (mg/g)	60.64±1.156	28.25–64.38	62.59	3.1
$Q_e \text{ PO}_4^{3-}$ ion (mg/g)	66.24±0.468	31.22–67.17	64.93	2.2

Furthermore, the control experiments were also conducted using actual poultry wastewater. The results are shown in Figure 7 with increase in biochar dosage. The actual wastewater had a concentration range of 92–436 mgNH₄⁺-N/L and 26–76 mgPO₄³⁻-P/L. The adsorption capacity of phosphate in actual wastewater (63.55±8.37 mgPO₄³⁻-P/g) was well in agreement with the predicted values (64.93 mgPO₄³⁻-P/g) while the adsorption capacity of the ammonium (47.41±0.3733 mgNH₄⁺-N/g) was not in good agreement with the predicted value of 62.59 mgNH₄⁺-N/g). It might be due to interference from other organic compounds in the wastewater, or by the charges of ammonium and biochar not suitable at the electrostatic attraction point [15]. In the research of Yin *et al.* [15] and Wang *et al.* [66], the removal efficiency of ammonium had a positive correlation with the acidic functional group. Moreover, the reduction of NH₄⁺ ions adsorptivity might have occurred because of the presence of cations (e.g., Mg²⁺, Fe³⁺, Zn²⁺, K⁺, Na⁺, and Ca²⁺), which are competitive for the active sites on the biochar surface [66]. Besides, since the adsorption capacity is calculated as mg of adsorbate on g of adsorbent, the higher the biochar dosage in the solutions, the lower the adsorption capacity of both ammonium and phosphate.

**Figure 7.** Actual wastewater experiment using BS biochar

4. Conclusions

MgO-impregnated biochar produced from waste bagasse and alum sludge had the ability to recover nutrients such as ammonia and phosphate from wastewater. Biochar is a cheap adsorption material and is highly effective, particularly after being impregnated with an MgCl₂ solution. The optimum values from the CCD design were determined, and were biochar dosage of 0.105 g/100 mL, initial

concentration of 90 mg/L, N/P ratio of 1.25, and pH 6. The highest adsorption capacities of the biochar in synthetic wastewater were 60.64 mgNH₄⁺-N/g and 66.24 mgPO₄³⁻-P/g. However, the ammonium adsorption capacity in the real wastewater experiment was lower than the predicted value from the model. In future work, biochar with other kinds of crop residues or impregnated with other metal oxides should be studied. Furthermore, a novel application of biochar after adsorptions could be its use as a slow-release fertilizer for soil application in the future.

5. Acknowledgements

We acknowledge the support of time and facilities from Ho Chi Minh City University of Technology (HCMUT), VNU-HCM for this study.

References

- [1] Diskowski, H. and Hofmann, T., 2000. *Phosphorus*. In: F. Ullmann, ed. *Ullmann's Encyclopedia of Industrial Chemistry*. New York: Wiley, pp. 725-746.
- [2] Dinh, X.T., 2017. *An Overview of Agricultural Pollution in Vietnam: The Livestock Sector*. [online] Available at: <https://openknowledge.worldbank.org/handle/10986/29244>.
- [3] Nguyen, H.T.Q., Le, T.K. and Nguyen, K.M., 2017. Agricultural residues biomass potential and applying efficiency for household scale biochar production in Go Cong Tay, Tien Giang province. *VNUHCM Journal of Earth Science and Environment*, 1(M1), 68-78, DOI: 10.32508/stdjsee.v1im1.429.
- [4] Chastain, J.P., Camberato, J.J. and Skewes, P., 2001. *Poultry Manure Production and Nutrient Content*. [online] Available at: https://www.clemson.edu/extension/camm/manuals/poultry/pch3b_00.pdf.
- [5] Yaakob, M.A., Mohamed, R.M.S.R., Al-Gheethi, A.A.S. and Kassim, A.H.M., 2018. Characteristics of chicken slaughterhouse wastewater. *Chemical Engineering Transactions*, 63, 637-642, DOI: 10.3303/CET1863107.
- [6] Rajakumar, R., Meenambal, T., Banu, J.R. and Yeom, I.T., 2011. Treatment of poultry slaughterhouse wastewater in upflow anaerobic filter under low upflow velocity. *International Journal of Environmental Science and Technology*, 8(1), 149-158, DOI: 10.1007/BF03326204.
- [7] Njoya, M., Basitere, M. and Ntwampe, S.K.O., 2019. Analysis of the characteristics of poultry slaughterhouse wastewater (PSW) and its treatability. *Water Practice and Technology*, 14(4), 959-970, DOI: 10.2166/WPT.2019.077.
- [8] Rauchfuss, T.B., 1996. *Phosphorus: An outline of its chemistry, biochemistry and technology*, fifth edition, studies in inorganic chemistry, #20 By D. E. C. Corbridge (University of Leeds). Elsevier: Amsterdam. *Journal of the American Chemical Society*, 118(33), 7871-7871, DOI: 10.1021/ja965522m.
- [9] Xue, Q., He, X., Sachs, S.D., Becker, G.C., Zhang, T. and Kruse, A., 2019. The current phosphate recycling situation in China and Germany: A comparative review. *Frontiers of Agricultural Science and Engineering*, 6(4), 403-418, DOI: 10.15302/J-FASE-2019287.
- [10] Shakoob, M.B., Ye, Z.L. and Chen, S., 2021. Engineered biochars for recovering phosphate and ammonium from wastewater: A review. *Science of the Total Environment*, 779, DOI: 10.1016/j.scitotenv.2021.146240.
- [11] Fang, C., Zhang, T., Li, P., Jiang, R.F. and Wang, Y.C., 2014. Application of magnesium modified corn biochar for phosphorus removal and recovery from swine wastewater.

- International Journal of Environmental Research and Public Health*, 11(9), 9217-9237, DOI: 10.3390/ijerph110909217.
- [12] GSO, 2020. *Analysis of Rice supply and demand in Vietnam*. [online] Available at: <https://www.gso.gov.vn/wp-content/uploads/2020/11/Ky-yeu-2019.pdf>. (in Vietnamese)
- [13] Vinitnantharat, S., Kositchaiyong, S. and Chiarakorn, S., 2010. Removal of fluoride in aqueous solution by adsorption on acid activated water treatment sludge. *Applied Surface Science*, 256(17), 5458-5462, DOI: 10.1016/J.APSUSC.2009.12.140.
- [14] Li, R., Wang, J.J., Zhou, B., Zhang, Z., Liu, S., Lei, S. and Xiao, R., 2017. Simultaneous capture removal of phosphate, ammonium and organic substances by MgO impregnated biochar and its potential use in swine wastewater treatment. *Journal of Cleaner Production*, 147, 96-107, DOI: 10.1016/j.jclepro.2017.01.069.
- [15] Yin, Q., Zhang, B., Wang, R. and Zhao, Z., 2017. Biochar as an adsorbent for inorganic nitrogen and phosphorus removal from water: a review. *Environmental Science and Pollution Research*, 24(34), 26297-26309, DOI: 10.1007/s11356-017-0338-y.
- [16] Castiglioni, M., Rivoira, L., Ingrand, I., Del Bubba, M. and Bruzzoniti, M.C., 2021. Characterization techniques as supporting tools for the interpretation of biochar adsorption efficiency in water treatment: A critical review. *Molecules*, 26(16), DOI: 10.3390/molecules26165063.
- [17] Zhang, Z., Huang, G., Zhang, P., Shen, J., Wang, S. and Li, Y., 2023. Development of iron-based biochar for enhancing nitrate adsorption: Effects of specific surface area, electrostatic force, and functional groups. *Science of The Total Environment*, 856, DOI: 10.1016/J.SCITOTENV.2022.159037.
- [18] Wang, X., Guo, Z., Hu, Z. and Zhang, J., 2020. Recent advances in biochar application for water and wastewater treatment: a review. *PeerJ*, 8, DOI: 10.7717/peerj.9164.
- [19] Luo, D., Wang, L., Nan, H., Cao, Y., Wang, H., Kumar, T.V. and Wang, C., 2023. Phosphorus adsorption by functionalized biochar: a review. *Environmental Chemistry Letters*, 21(1), 497-524, DOI: 10.1007/s10311-022-01519-5.
- [20] Ren, J., Li, N., Li, L., An, J.-K., Zhao, L. and Ren, N.-Q., 2015. Granulation and ferric oxides loading enable biochar derived from cotton stalk to remove phosphate from water. *Bioresource Technology*, 178, 119-125, DOI: 10.1016/j.biortech.2014.09.071.
- [21] Cai, G. and Ye, Z.-L., 2022. Concentration-dependent adsorption behaviors and mechanisms for ammonium and phosphate removal by optimized Mg-impregnated biochar. *Journal of Cleaner Production*, 349, DOI: 10.1016/j.jclepro.2022.131453.
- [22] Yin, Q., Liu, M. and Ren, H., 2019. Removal of ammonium and phosphate from water by Mg-modified biochar: Influence of Mg pretreatment and pyrolysis temperature. *BioResources*, 14(3), 6203-6218, DOI: 10.15376/biores.14.3.6203-6218.
- [23] Xu, K., Lin, F., Dou, X., Zheng, M., Tan, W. and Wang, C., 2018. Recovery of ammonium and phosphate from urine as value-added fertilizer using wood waste biochar loaded with magnesium oxides. *Journal of Cleaner Production*, 187, 205-214, DOI: 10.1016/j.jclepro.2018.03.206.
- [24] Serra-Toro, A., Astals, S., Madurga, S., Mata-Ivarez, J., Mas, F. and Dosta, J., 2022. Ammoniacal nitrogen recovery from pig slurry using a novel hydrophobic/hydrophilic selective membrane. *Journal of Environmental Chemical Engineering*, 10(5), DOI: 10.1016/j.jece.2022.108434.
- [25] Company, E., Farris, M., Colprim, J. and Magr, A. 2022. Exploring the recovery of potassium-rich struvite after a nitrification-denitrification process in pig slurry treatment. *Science of the Total Environment*, 847, DOI: 10.1016/j.scitotenv.2022.157574.
- [26] Romero-Giza, M.S., Tait, S., Astals, S., del Valle-Zermeo, R., Martinez, M., Mata-Alvarez, J. and Chimenos, J.M., 2015. Reagent use efficiency with removal of nitrogen from pig slurry via struvite: A study on magnesium oxide and related by-products. *Water Research*, 84, 286-294, DOI: 10.1016/J.WATRES.2015.07.043.
- [27] He, L., Wang, D., Wu, Z., Lv, Y. and Li, S., 2022. Magnesium-modified biochar was used to adsorb phosphorus from wastewater and used as a phosphorus source to be recycled to reduce

- the ammonia nitrogen of piggery digestive wastewater. *Journal of Cleaner Production*, 360, DOI: 10.1016/j.jclepro.2022.132130.
- [28] Zin, M.M.T. and Kim, D.-J., 2021. Simultaneous recovery of phosphorus and nitrogen from sewage sludge ash and food wastewater as struvite by Mg-biochar. *Journal of Hazardous Materials*, 403, DOI: 10.1016/j.jhazmat.2020.123704.
- [29] Santhosh, C., Daneshvar, E., Tripathi, K.M., Baltrėnas, P., Kim, T.Y., Baltrėnaitė, E. and Bhatnagar, A., 2020. Synthesis and characterization of magnetic biochar adsorbents for the removal of Cr(VI) and acid orange 7 dye from aqueous solution. *Environmental Science and Pollution Research*, 27(22), 32874-32887, DOI: 10.1007/S11356-020-09275-1.
- [30] Jiang, Y.H., Li, A.Y., Deng, H., Ye, C.H., Wu, Y.Q., Linmu, Y.D. and Hang, H.L., 2019. Characteristics of nitrogen and phosphorus adsorption by Mg-loaded biochar from different feedstocks. *Bioresource Technology*, 276, 183-189, DOI: 10.1016/j.biortech.2018.12.079.
- [31] Kończak, M. and Huber, M., 2022. Application of the engineered sewage sludge-derived biochar to minimize water eutrophication by removal of ammonium and phosphate ions from water. *Journal of Cleaner Production*, 331, DOI: 10.1016/j.jclepro.2021.129994.
- [32] He, Q., Li, X. and Ren, Y., 2022. Analysis of the simultaneous adsorption mechanism of ammonium and phosphate on magnesium-modified biochar and the slow release effect of fertiliser. *Biochar*, 4, DOI: 10.1007/s42773-022-00150-5.
- [33] Xi, H., Zhang, X., Zhang, A.M., Guo, F., Yang, Y., Lu, Z., Ying, G. and Zhang, J., 2022. Concurrent removal of phosphate and ammonium from wastewater for utilization using Mg-doped biochar/bentonite composite beads. *Separation and Purification Technology*, 285, DOI: 10.1016/j.seppur.2021.120399.
- [34] Lehmann, J. and Joseph, S., 2009. *Biochar for Environmental Management*. London: Routledge.
- [35] Rajakumar, R., Meenambal, T., Banu, J.R. and Yeom, I.T., 2010. Treatment of poultry slaughterhouse wastewater in upflow anaerobic filter under low upflow velocity. *International Journal of Environment Science and Technology*, 8, 149-158, DOI: 10.1007/BF03326204.
- [36] Chavez, P.C., Castillo, L.R., Dendooven, L. and Escamilla-Silva, E.M., 2005. Poultry slaughter wastewater treatment with an up-flow anaerobic sludge blanket (UASB) reactor. *Bioresource Technology*, 96(15), 1730-1736, DOI: 10.1016/j.biortech.2004.08.017.
- [37] Yao, Y., Gao, B., Chen, J. and Yang, L., 2013. Engineered biochar reclaiming phosphate from aqueous solutions: Mechanisms and potential application as a slow-release fertilizer. *Environmental Science and Technology*, 47(15), 8700-8708, DOI: 10.1021/es4012977.
- [38] Xu, K., Li, J., Zheng, M., Zhang, C., Xie, T. and Wang, C., 2015. The precipitation of magnesium potassium phosphate hexahydrate for P and K recovery from synthetic urine. *Water Research*, 80, 71-79, DOI: 10.1016/j.watres.2015.05.026.
- [39] Takaya, C.A., Fletcher, L.A., Singh, S. and Okwuosa, U.C. and Ross, A.B., 2016. Recovery of phosphate with chemically modified biochars. *Journal of Environmental Chemical Engineering*, 4(1), 1156-1165, DOI: 10.1016/j.jece.2016.01.011.
- [40] Zhang, Y., Li, Z. and Mahmood, I.B., 2014. Recovery of NH_4^+ by corn cob produced biochars and its potential application as soil conditioner. *Frontiers of Environmental Science and Engineering* 8(6), 825-834, DOI: 10.1007/S11783-014-0682-9.
- [41] Ajmal, Z., Muhmood, A., Dong, R. and Wu, S., 2020. Probing the efficiency of magnetically modified biomass-derived biochar for effective phosphate removal. *Journal of Environmental Management*, 253, DOI: 10.1016/j.jenvman.2019.109730.
- [42] Michlekov, R., 2017. Iron-impregnated biochars as effective phosphate sorption materials. *Environmental Science and Pollution Research*, 24(1), 463-475, DOI: 10.1007/s11356-016-7820-9.
- [43] Dai, Y., Wang, W., Lu, L., Yan, L. and Yu, D., 2020. Utilization of biochar for the removal of nitrogen and phosphorus. *Journal of Cleaner Production*, 257, DOI: 10.1016/j.jclepro.2020.120573.

-
- [44] Zhang, H., Voroney, R.P. and Price, G.W., 2015. Effects of temperature and processing conditions on biochar chemical properties and their influence on soil C and N transformations. *Soil Biology and Biochemistry*, 83, 19-28, DOI: 10.1016/j.soilbio.2015.01.006.
 - [45] Zhang, Z., Yan, L., Yu, H., Yan, T. and Li, X., 2019. Adsorption of phosphate from aqueous solution by vegetable biochar/layered double oxides: Fast removal and mechanistic studies. *Bioresource Technology*, 284, 65-71, DOI: 10.1016/j.biortech.2019.03.113.
 - [46] Wang, Z., Wang, S., Bian, T., Song, Q., Wu, G., Awais, M., Liu, Y., Fu, H. and Sun, Z., 2022. Effects of nitrogen addition on soil microbial functional diversity and extracellular enzyme activities in greenhouse cucumber cultivation. *Agriculture*, 12(9), DOI: 10.3390/agriculture12091366.
 - [47] Fang, L., shan Li, J., Donatello, S., Cheeseman, C.R., Poon, C.S. and Tsang, D.C.W., 2020. Use of Mg/Ca modified biochars to take up phosphorus from acid-extract of incinerated sewage sludge ash (ISSA) for fertilizer application. *Journal of Cleaner Production*, 244, DOI: 10.1016/j.jclepro.2019.118853.
 - [48] Wang, B., Ma, Y., Lee, X., Wu, P., Liu, F., Zhang, X., Li, L. and Chen, M., 2021. Environmental-friendly coal gangue-biochar composites reclaiming phosphate from water as a slow-release fertilizer. *Science of The Total Environment*, 758, DOI: 10.1016/j.scitotenv.2020.143664.
 - [49] Wang, C., Sun, R. and Huang, R., 2021. Highly dispersed iron-doped biochar derived from sawdust for Fenton-like degradation of toxic dyes. *Journal of Cleaner Production*, 297, DOI: 10.1016/j.jclepro.2021.126681.
 - [50] Melia, P.M., Busquets, R., Hooda, P.S., Cundy, A.B. and Sohi, S.P., 2019. Driving forces and barriers in the removal of phosphorus from water using crop residue, wood and sewage sludge derived biochars. *Science of The Total Environment*, 675, 623-631, DOI: 10.1016/j.scitotenv.2019.04.232.
 - [51] Afagwu, C., Mahmoud, M., Alafnan, S., Alqubalee, A., ElHusseiny, A. and Patil, S., 2022. Pore volume characteristics of clay-rich shale: Critical insight into the role of clay types, aluminum and silicon concentration. *Arabian Journal for Science and Engineering*, 47(9), 12013-12029, DOI: 10.1007/S13369-022-06720-w.
 - [52] Zhang, Y., Shao, D., Yan, J., Jia, X., Li, Y., Yu, P. and Zhang, T., 2016. The pore size distribution and its relationship with shale gas capacity in organic-rich mudstone of Wufeng-Longmaxi Formations, Sichuan Basin, China. *Journal of Natural Gas Geoscience*, 1(3), 213-220, DOI: 10.1016/j.jnggs.2016.08.002.
 - [53] Sing, K.S.W. and Williams, R.T., 2016. Physisorption hysteresis loops and the characterization of nanoporous materials. *Adsorption Science and Technology*, 22(10), 773-782, DOI: 10.1260/0263617053499032.
 - [54] Jia, L., Niu, B., Jing, X. and Wu, Y., 2022. Equilibrium and hysteresis formation of water vapor adsorption on microporous adsorbents: Effect of adsorbent properties and temperature. *Journal of the Air and Waste Management Association*, 72(2), 176-186, DOI: 10.1080/10962247.2021.2011477.
 - [55] Muduli, R.C. and Kale, P., 2022. Chemically modified surface of silicon nanostructures to enhance hydrogen uptake capabilities. *International Journal of Hydrogen Energy*, DOI: 10.1016/j.ijhydene.2022.06.030.
 - [56] Le, V.G., Vo, D.V.N., Nguyen, N.H., Shih, Y.J., Vu, C.T., Liao, C.H. and Huang, Y.H., 2021. Struvite recovery from swine wastewater using fluidized-bed homogeneous granulation process. *Journal of Environmental Chemical Engineering*, 9(3), DOI: 10.1016/j.jece.2020.105019.
 - [57] Kubar, A.A., Huang, Q., Sajjad, M., Yang, C., Lian, F., Wang, J. and Kubar, K.A., 2021. The recovery of phosphate and ammonium from biogas slurry as value-added fertilizer by biochar and struvite co-precipitation. *Sustainability*, 13(7), DOI: 10.3390/su13073827.
 - [58] Li, X., Zhao, X., Zhou, X. and Yang, B., 2021. Phosphate recovery from aqueous solution via struvite crystallization based on electrochemical-decomposition of nature magnesite. *Journal of Cleaner Production*, 292, DOI: 10.1016/j.jclepro.2021.126039.

- [59] Folino, A., Zema, D.A. and Calabrò, P.S., 2020. Environmental and economic sustainability of swine wastewater treatments using ammonia stripping and anaerobic digestion: A short review. *Sustainability*, 12(12), DOI: 10.3390/su12124971.
- [60] Zhang, J. and Wang, Q., 2016. Sustainable mechanisms of biochar derived from brewers' spent grain and sewage sludge for ammonia–nitrogen capture. *Journal of Cleaner Production*, 112, 3927-3934, DOI: 10.1016/j.jclepro.2015.07.096.
- [61] Li, R., Wang, J.J., Zhou, B., Awasthi, M.K., Ali, A., Zhang, Z., Gaston, L.A., Lahori, A.H. and Mahar, A., 2016. Enhancing phosphate adsorption by Mg/Al layered double hydroxide functionalized biochar with different Mg/Al ratios. *Science of the Total Environment*, 559, 121-129, DOI: 10.1016/j.scitotenv.2016.03.151.
- [62] Moradi, M., Fazlzadehdavil, M., Pirsaeheb, M., Mansouri, Y., Khosravi, T. and Sharafi, K., 2016. Response surface methodology (RSM) and its application for optimization of ammonium ions removal from aqueous solutions by pumice as a natural and low cost adsorbent. *Archives of Environmental Protection*, 42(2), 33-43, DOI: 10.1515/aep-2016-0018.
- [63] Barbosa, S.G., Peixoto, L., Meulman, B., Alves, M.M. and Pereira, M.A., 2016. A design of experiments to assess phosphorous removal and crystal properties in struvite precipitation of source separated urine using different Mg sources. *Chemical Engineering Journal*, 298, 146-153, DOI: 10.1016/j.cej.2016.03.148.
- [64] Deem, L.M. and Crow, S.E., 2017. Biochar. In: S. Elias, ed. *Reference Module in Earth Systems and Environmental Sciences*. Amsterdam: Elsevier.
- [65] Zhang, M., Song, G., Gelardi, D.L., Huang, L., Khan, E., Masek, O., Parikh, S.J. and Ok, Y.S., 2020. Evaluating biochar and its modifications for the removal of ammonium, nitrate, and phosphate in water. *Water Research*, 186, DOI: 10.1016/j.watres.2020.116303.
- [66] Wang, Z., Guo, H., Shen, F., Yang, G., Zhang, Y., Zeng, Y., Wang, L., Xiao, H. and Deng, S., 2015. Biochar produced from oak sawdust by Lanthanum (La)-involved pyrolysis for adsorption of ammonium (NH_4^+), nitrate (NO_3^-), and phosphate (PO_4^{3-}). *Chemosphere*, 119, 646-653. DOI: 10.1016/j.chemosphere.2014.07.084.
- [67] Sarkhot, D.V., Ghezzehei, T.A. and Berhe, A.A., 2013. Effectiveness of biochar for sorption of ammonium and phosphate from dairy effluent. *Journal of Environmental Quality*, 42(5), 1545-1554, DOI: 10.2134/jeq2012.0482.
- [68] Yin, Q., Zhang, B., Wang, R. and Zhao, Z., 2017. Phosphate and ammonium adsorption of sesame straw biochars produced at different pyrolysis temperatures. *Environmental Science and Pollution Research*, 25(5), 4320-4329, DOI: 10.1007/s11356-017-0778-4.
- [69] Jung, K.W. and Ahn, K.H., 2016. Fabrication of porosity-enhanced MgO/biochar for removal of phosphate from aqueous solution: Application of a novel combined electrochemical modification method. *Bioresource Technology*, 200, 1029-1032. DOI: 10.1016/j.biortech.2015.10.008.